The Use of Extracorporeal Shock Wave-Stimulated Periosteal Cells for Orthotopic Bone Generation

TISSUE ENGINEERING: Part A
Volume 18, Numbers 13 and 14, 2012

DOI: 10.1089/ten.tea.2011.0573

The Use of Extracorporeal Shock Wave-Stimulated Periosteal Cells for Orthotopic Bone Generation

Cathal J. Kearney, Ph.D.,[1,2] Huping P. Hsu, M.D.,[2,3] and Myron Spector, Ph.D.[1–3]

The cambium cells of the periosteum, which are known osteoprogenitor cells, have limited suitability for clinical applications of tissue engineering in their native state due to their low cell number (2–5 cells thick). Extracorporeal shock waves (ESWs) have been shown to cause rapid periosteal cambium cell proliferation and subsequent periosteal osteogenesis. This work investigates a novel strategy for orthotopic bone generation: applying ESW therapy as a noninvasive, inexpensive, and rapid method for stimulating cambium cell proliferation, and combining these cells with a bioactive scaffold for bone growth. ESWs applied to the rabbit medial tibia resulted in a significant 2.7-fold increase in cambium cell number and a 4-fold increase in cambium cell thickness at 4 days post-ESW. ESW-stimulated, or nontreated control, periosteal cells were elevated *in situ* and overlaid on an anorganic bovine bone scaffold to interrogate their ability to form bone. At 2 weeks post-surgery, there was a significant increase in all key outcome variables for the ESW-stimulated group when compared with controls: a 4-fold increase in osseous tissue in the upper half of the scaffold underlying the periosteum; a 12-fold increase in osseous tissue overlying the scaffold; and a 2-fold increase in callus size. These results successfully demonstrated the efficacy of ESW-stimulated periosteum for orthotopic bone generation.

Introduction

Bone is a regenerative tissue that is capable of osseous regeneration in fractures and contained defects due, in part, to its vascular network, reservoir of osteoprogenitor cells, and its constant turnover throughout life[1]; however, its capability for orthotopic regeneration is limited, as there is an insufficient framework for tissue repair.[2–6] The current clinical gold standard is to treat these defects with autografts; however, autografts are known to undergo resorption at the treatment site, cause morbidity at the harvest site, and the volume that can be treated is limited in size by the available harvest volume.[2,3,5,7] Furthermore, autografting requires an additional surgical procedure, and this may be technically challenging in certain situations (e.g., a dental surgeon requiring non-oral bone source).[3,5]

There have been numerous approaches for treating these defects with various tissue-engineering strategies, which combine one or more components of the tissue-engineering triad: cells, scaffolds, and growth factors.[2–6,8] *In vitro* tissue generation before implantation is advantageous, as the culture environment, shape, and load bearing can be carefully controlled.[2–6,8] However, these strategies are expensive; moreover, there are technical challenges that are associated with implantation (especially for larger defects): maintaining cell viability, revascularizing the tissue, and integrating the tissue biologically and mechanically.[4,6] *In vivo* engineering of bone using strategies that combine porous ceramic or demineralized bone scaffolds with marrow-derived mesenchymal stem cells and/or bone morphogenetic proteins has been more successful.[2–6] However, these strategies can be complex and costly, and they require careful management.

The periosteum, long employed as an autograft for bone and cartilage procedures, is comprised of two layers of tissue: the inner cambium layer, which consists of progenitor cells, and the outer fibrous layer comprising fibroblasts. Periosteal cambium cells are promising for bone tissue-engineering applications because of their ability to proliferate, their osteogenic potential, and their accessibility.[9–12] The ability of periosteal cells to differentiate into multiple cell types (osteoblast, chondrocyte, adipocyte, and myocyte) has been demonstrated both *in vivo* and *in vitro*, which demonstrates the value of this cell source.[13] The thinness of the periosteum can be advantageous, as it can be quickly revascularized after transplantation; however, for applications dependent on its progenitor cells, the periosteum is typically limited by its low cell number (a cambium layer that is 2–5 cells thick), and consequently its thickness makes harvest technically difficult.[14] To overcome this drawback, various

[1]Harvard-MIT Division of Health Sciences and Technology, Massachusetts Institute of Technology, Cambridge, Massachusetts.
[2]Tissue Engineering Laboratory, Veterans Administration Boston Healthcare System, Boston, Massachusetts.
[3]Orthopaedic Research Laboratory, Brigham and Women's Hospital, Harvard Medical School, Boston, Massachusetts.

strategies have been developed to increase the cambium cell number by surgical trauma, culture, or growth factor injection.[9,12,15–18]

Although there are many non-invasive energy sources (*e.g.*, thermal, acoustic, and laser) that are known to have stimulatory effects on cells, there are a few examples of tissue-engineering strategies which utilize these techniques to stimulate cells *in vivo* before combining them with a scaffold for tissue generation. Our previous work demonstrated the ability of extracorporeal shock waves (ESWs) to rapidly stimulate cambium cell proliferation and the osteogenic differentiation of these cells.[19] Herein, we describe a novel approach to orthotopic bone generation that combines extracorporeal shock wave-stimulated periosteum (ESWSP) with a porous osteoconductive scaffold (see Fig. 1).

In a rabbit model, we compared the control periosteum (CP) to ESWSP with and without scaffold implantation (see Table 1 for experimental design). Animals were sacrificed either 4 days post-ESW stimulation or 2 weeks after scaffold implantation, and were qualitatively evaluated using microcomputed tomography (micro-CT). Histology was performed on decalcified sections from all groups, and a histomorphometric analysis was performed to quantify the tissue response.

Materials and Methods

Experimental design

All procedures were approved by the Veterans Administration (VA) Boston Healthcare System Institutional Animal Care and Use Committee. Eighteen adult New Zealand White rabbits (4–4.5 kg) were used in total, divided into three groups (groups 2–4) as described in Table 1. A fourth group comprised the untreated contralateral limbs from group 2. All groups were designed to have $n=6$. The power calculation was based on determining as significant a difference between the treated and control limbs of 30% for select outcome variables, assuming a standard deviation of 15% and $\alpha=\beta=0.05$.

Shock wave application

The shock wave treatment was based on our findings in rat studies.[19] The focused ESW treatment was applied using the OssaTron (SANUWAVE Health, Inc., Alpharetta, GA) operating at 28 kV (energy flux density of 0.40 mJ/mm^2; ellipsoid focal zone ~1 cm diameter × 7 cm long). The rabbits were anesthetized using ketamine (10 mg/kg) and acepromazine (0.5 mg/kg) for induction and maintained with isoflurane (1–2% by endotracheal intubation) and O_2 throughout the procedure. The pressure in the treatment head was adjusted to ensure the secondary focus was centered at the applicator tip, which was coupled to the shaved medial proximal tibia using ultrasound gel (Fig. 1B). The device was oriented perpendicular to the rabbit tibia along the centerline of the medial aspect of the tibia at 17.5 mm distal to the center of the knee joint. Overall, 3000 shocks were delivered (4 s^{-1}) in one treatment session. Ketofen (2 mg/kg) was subcutaneously administered for 24 h post-ESW.

Scaffold preparation

The calcium phosphate scaffolds used in this study were anorganic bovine cancellous bone with pore sizes distributed from 200 to 800 μm. The scaffolds were obtained as blocks (Geistlich Pharma, Wolhusen, Switzerland), sliced 1.6 cm

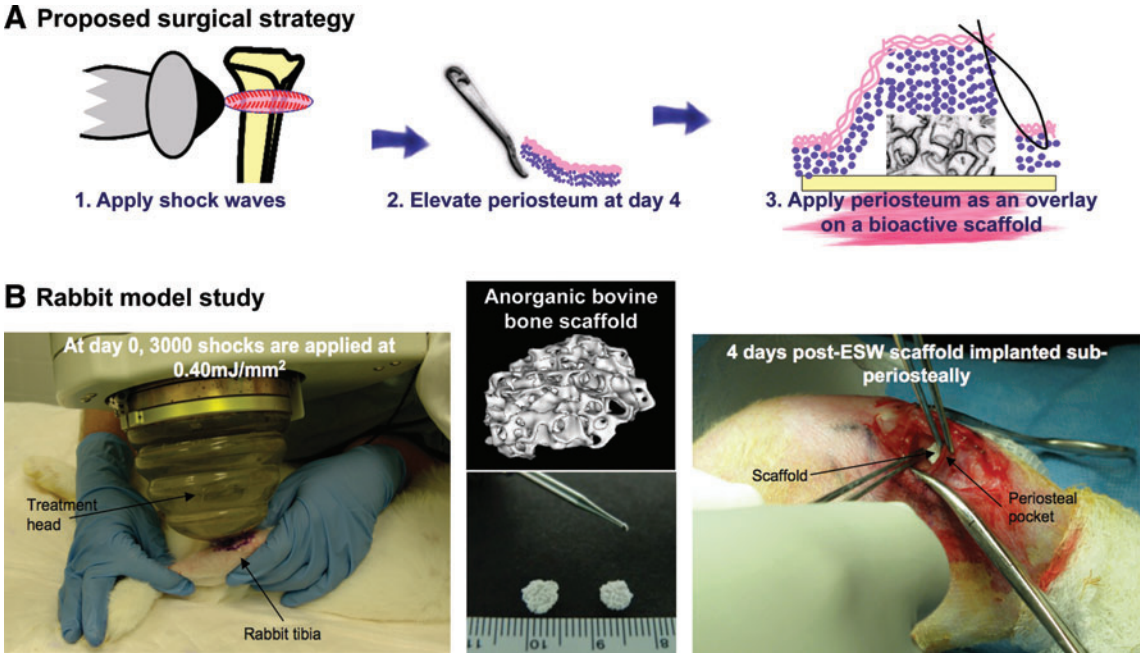

FIG. 1. Proposed strategy for orthotopic bone generation. **(A)** Overview of strategy: the periosteal cell source at the defect site is stimulated with extracorporeal shock waves 4 days before surgery. At the time of surgery, the cells are elevated off the bone, and a subperiosteal scaffold is implanted. **(B)** Images of the various stages as performed in the rabbit study. ESW, extracorporeal shock waves. Color images available online at www.liebertonline.com/tea

Table 1. Table of Experimental Groups

Experimental group	*Treatment*	*ESW*	*Surgery*	n
Group 1	**CP:** Untreated contralateral limbs from group 2 rabbits	None	N	6
Group 2	**ESWSP:** Animals are sacrificed 4 days post–ESW	3000 shocks @ 0.4 mJ/mm^2	N	6
Group 3	**CP+scaffold:** Scaffold was implanted under normal periosteum (medial proximal tibia). Animals are sacrificed at 2 weeks postop	None	Y	6
Group 4	**ESWSP+scaffold:** At day 4 post-ESW, scaffold is implanted under ESW-treated periosteum (medial proximal tibia). Animals are sacrificed at 2 weeks postop	3000 shocks @ 0.4 mJ/mm^2	Y	6

ESWSP, extracorporeal shock wave stimulated periosteum; CP, control periosteum.

thick by using a diamond saw (Buehler Isomet, Lake Bluff, IL), and trimmed to 5.5 mm diameter using a burr. The scaffolds were sterilized with STERRAD sterilization system (Irvine, CA).

Surgery

The rabbits were anesthetized as described for ESW, and all procedures were carried out under sterile conditions. A 1.5 cm skin incision was made above the ESW application site and using a scalpel, the periosteum was scored in an arc proximal to the implant site. A periosteal elevator was used to elevate the periosteum and to scrape the cortical surface clean of cambium cells. The scaffold was implanted in the surgically created periosteal pocket, and the periosteum was sutured closed. Ketofen (2 mg/kg) and cefazolin (20 mg/kg) were given subcutaneously for 48 h post-op, and the animals were sacrificed at 2 weeks post-op.

Micro-CT analysis and tissue processing

After sacrifice, the implants and surrounding bone were excised and imaged using micro-CT (GE Healthcare eXplore Locus; 27 μm, 88 min Short Scan; GE Healthcare, Piscataway, NJ). Subsequently, the samples were fixed in formalin and decalcified using 10% formic acid before paraffin embedding. Using a microtome, axial cross-sections were removed at 1 mm increments along the bone. Slides were stained with hematoxylin and eosin and Safranin O, and examined under light microscopy.

Histomorphometric analysis

The histological sections clearly demarcated the tissue types and were used for analysis—the micro-CT images did not show the immature unmineralized tissue, and the mature tissue was of a similar radiodensity as the implant.

In groups 1 and 2, two slides 1 mm apart—coincident with the implant site—were analyzed. Cell counts were taken in an area 50 μm wide (along the circumference of the periosteum) and through the entire thickness of the cambium layer; this analysis has been described previously as a way to compare periosteal thickness.[19] Three cell counts were taken per slide—medial tibia centerline and at ± 1.5 mm. Data were recorded from digitized images using ImageJ (NIH; http://rsbweb.nih.gov/ij/).

For groups 3 and 4, the two centermost scaffold sections (1 mm apart) were analyzed in ImageJ. The total callus on the medial side, which included all tissue inside the periosteal pocket up to the cortical surface and the tissues above the scaffold, were recorded. The periosteal callus away from the scaffold, which demonstrated the various stages of endochondral ossification, served as an internal control for tissue appearance during histogenesis. Tissue reported as "osteoprogenitor" tissue included any areas that had already committed to forming, or that had formed, bone; the remaining tissue was classified as non-osteoprogenitor. The osteoprogenitor tissue was further subdivided into osseous tissue (immature and maturing bone) and chondrocytic tissue (hyaline cartilage and hypertrophic/calcifying chondrocytes).

To eliminate edge effects, an area with a width of 50% of the scaffold implant thickness was excluded on both sides. The scaffold was subdivided into the upper (response to the elevated periosteum) and lower half (response to cells remaining on the cortical surface), the porous area was demarcated, and the tissue areas were recorded.

The areal amounts of the various tissue types were normalized to the areas of the selected regions to yield percentages, because of the variations (albeit slight) in scaffold architecture and size among animals. The absolute values for the areal amounts of the various tissue types are included in the Supplementary Table S1 (Supplementary Data are available online at www.liebertonline.com/tea).

Statistical analysis

All data are reported as the mean ± SEM of all the animals for each group. The two-tailed Student's *t*-test was used to compare groups, and *p*-values of <0.05 were considered significant.

Results

Groups 1 versus 2: CP versus ESWSP (no scaffold implanted)

We first tested the effectiveness of an ESW dose that we had previously used to demonstrate periosteal proliferation in rats,[19] to stimulate cambium cell proliferation in rabbits. The bases for establishing that it was cells within the cambium layer that had proliferated in this and our previous study in rats[19] included (1) the location of the cells near the bone surface instead of in the fibrous layer away from the bone surface; (2) the absence of an elongated morphology consistent with the fibroblasts in the fibrous layer; and (3) the

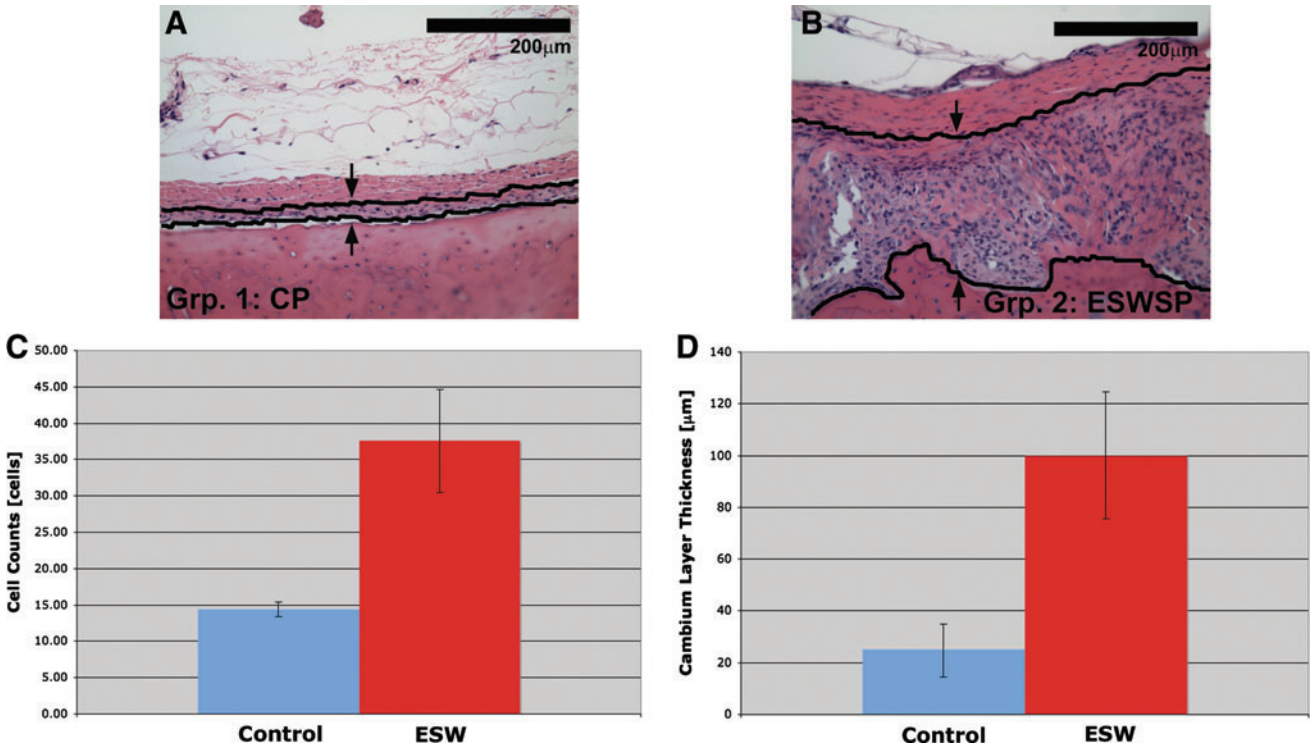

FIG. 2. Micrographs of periosteum from **(A)** control and **(B)** ESW-stimulated periosteum (ESWSP) samples at day 4, which demonstrate the proliferation of the cambium layer cells (black outlines and arrows) in response to ESWs. Graphs of control and ESWSP **(C)** cell counts and **(D)** cambium layer thickness, which quantify the proliferative effect of ESWs ($n=6$; mean ± SEM). Color images available online at www.liebertonline.com/tea

osteogenic nature of the cells as reflected in the subsequent presence of bone at the location of the proliferating cells. In five of the six shock wave-stimulated tibiae, there was a marked thickening of the periosteum (see Fig. 2). There was a four-fold, statistically significant increase in the thickness of the ESWSP when compared with the contralateral, non-stimulated controls ($100 \pm 24.7\,\mu m$ vs. $25 \pm 2.3\,\mu m$; $p=0.013$). There was also a significant 2.7-fold increase in periosteal cell number when compared with controls (38 ± 7 vs. 14 ± 1; $p=0.008$). The width—along the medial side of the tibia in group 2 samples—of this proliferated layer of cambium cells was $8.7 \pm 0.5\,mm$, which closely matches the devices' focal zone diameter. Micro-CT imaging ($n=4$) did not demonstrate any changes on the medial side; however, three of the four ESW samples demonstrated small healing micro-fractures on the postero-lateral corner (the side opposite ESW application), which was not seen in controls.

Groups 3 versus 4: CP + scaffold versus ESWSP + scaffold

After verifying the effectiveness of the selected ESW dose to stimulate rapid cambium cell proliferation, we next elevated ESWSP at day 4 and overlaid it on an anorganic bovine bone scaffold that had previously been shown to form bone when combined with cambium cells.[20]

There was no evidence of bone formation above the scaffold in five of the six samples in the control group (one sample demonstrated a small cartilage nodule above the scaffold); the sixth sample had a thin layer of bone above the scaffold. This sample showed some endochondral ossification within the scaffold pores; in the five other control rabbits, the scaffolds were filled with nonosteoprogenitor tissue that was typically fibrous (see Fig. 3). Some filling of the scaffold lower halves with osteoprogenitor tissue was contributed from cells on the cortical surface.

During one of the surgeries of the group 4 samples, the periosteum tore and, as a consequence of contraction, a much smaller scaffold was implanted. Due to the dramatic differences in this animal's surgery, this sample was excluded from analysis.

For group 4 samples, there was periosteal callus on both sides of the scaffold that was undergoing osteogenesis and was continuous with osteogenic tissue over the scaffold (see Fig. 3). This tissue was primarily undergoing endochondral ossification, and it ranged in maturity from hyaline cartilage to trabecular bone. In contrast to controls, the upper half of the scaffold had osteoprogenitor tissue infiltrating the scaffold from the overlaid periosteum (see Fig. 3). The tissue in the upper pores was continuous with the tissue forming in the lower pores; however, as with the control samples, there also appeared to be bone formed by progenitor cells left over after scraping the cortical surface (see Fig. 3).

At the edge closest to the intact end of the periosteum, both CP and ESWSP samples demonstrated relatively more mature osseous tissue; at the sutured end, there was more fibrous tissue formation. On micro-CT, it was recorded that in four of the five ESWSP samples, the periosteum had

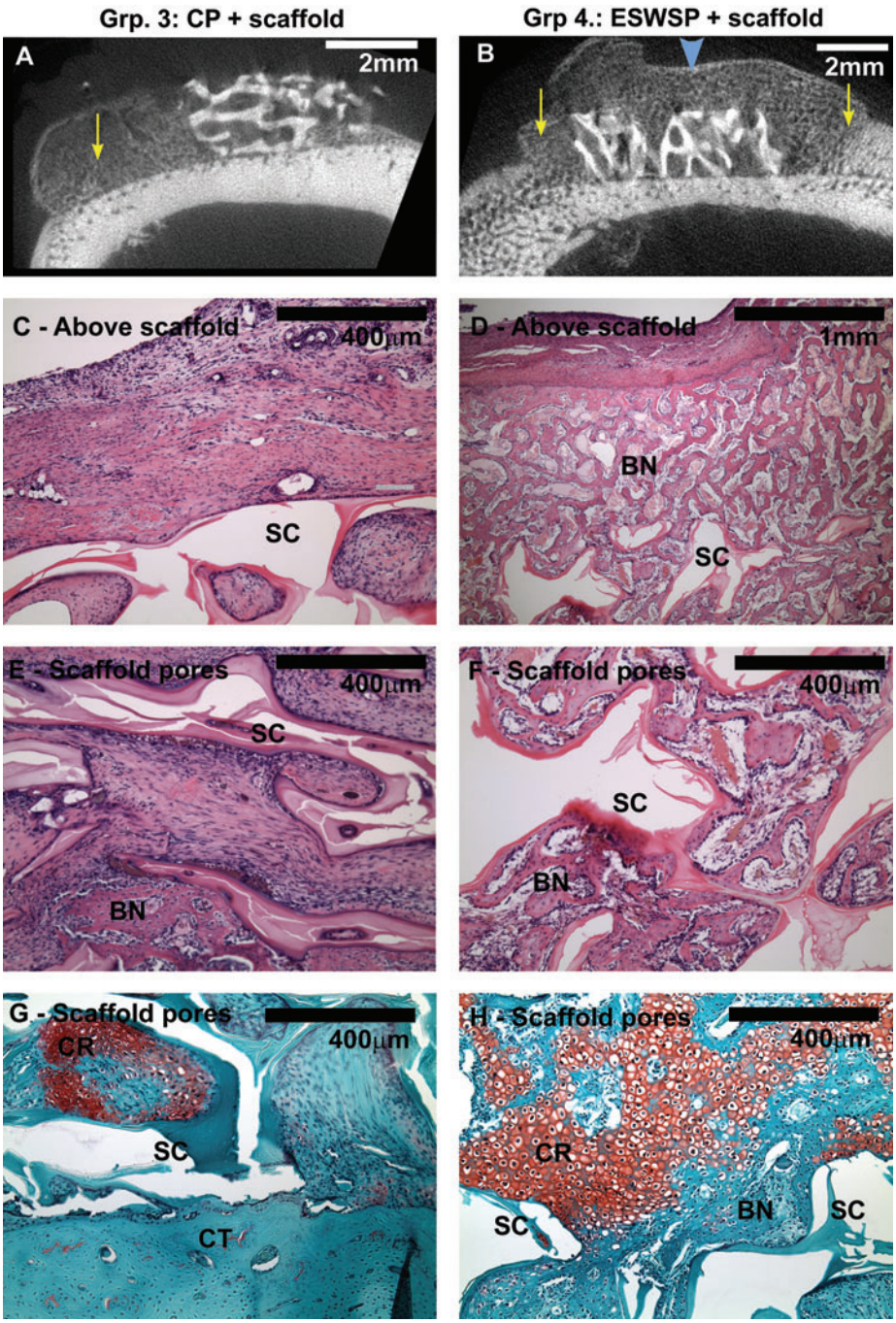

FIG. 3. Sample images from the control surgery group **(**group 3: control periosteum [CP]+ scaffold; **A, C, E, G)** and ESWSP surgery group **(**group 4: ESWSP+scaffold; **B, D, F, H)**. **(A, B)** Sample of axial cross-section microcomputed tomography images at scaffold center (yellow arrows—periosteal proliferation in response to surgical elevation±ESWs; blue arrowheads—periosteal response above scaffold in ESWSP group). **(C–H)** Sample histological micrographs of reparative tissue for control samples and ESWSP samples. Control samples demonstrated little bone formation above the scaffold **(C),** and the only bone formation in the scaffold came from cells on the cortical bone surface **(**at base of micrograph **E** and **G)**. ESW-stimulated periosteal cells demonstrated robust osseous and osteoprogenitor (undergoing endochondral ossification) tissue above **(D)** and within **(F)** the scaffold. (BN, bone; CR, cartilage; CT, cortical bone; SC, scaffold). The Safranin O stains demonstrate cartilage formation, which precedes endodchondral ossification, in both groups **(G, H)**. Note that some scaffold was lost during histological processing, leaving voids. Color images available online at www.liebertonline.com/tea

longitudinally contracted; however, coverage was typically 75% (the lack of osteogenic tissue precluded this measurement from being made in group 3). Three of the five ESWSP samples had evidence of healing microfractures on micro-CT on the postero-lateral side (side opposite ESW application); the other two samples demonstrated periosteal callus formation at this site, but no microfractures were seen on micro-CT.

Histomorphometric analysis

For the ESWSP group, the upper half of the scaffold underlying the periosteum had an almost fourfold increase in the percent of osseous tissue filling the scaffold pores, which was statistically significant (see Fig. 4A; 58%±13% vs. 15%±5%; $p=0.008$). When the chondrocytic tissue was also considered (Fig. 4B), there was a 3.3-fold increase in osteoprogenitor tissue (osseous + chondrocytic tissue) when compared with controls, with almost three-quarters of the scaffold in the ESW-treated samples filled with osteoprogenitor tissue (74%±8% vs. 22%±5%; $p=0.003$). In contrast to the upper half of the scaffold, there was no difference between the ESWSP and CP groups for the lower half of the scaffold, apposed to the bone surface, for either osseous tissue (44%±15% vs. 43%±8%; $p=0.94$) or osteoprogenitor tissue (46%±15% vs. 45%±8%; $p=0.94$).

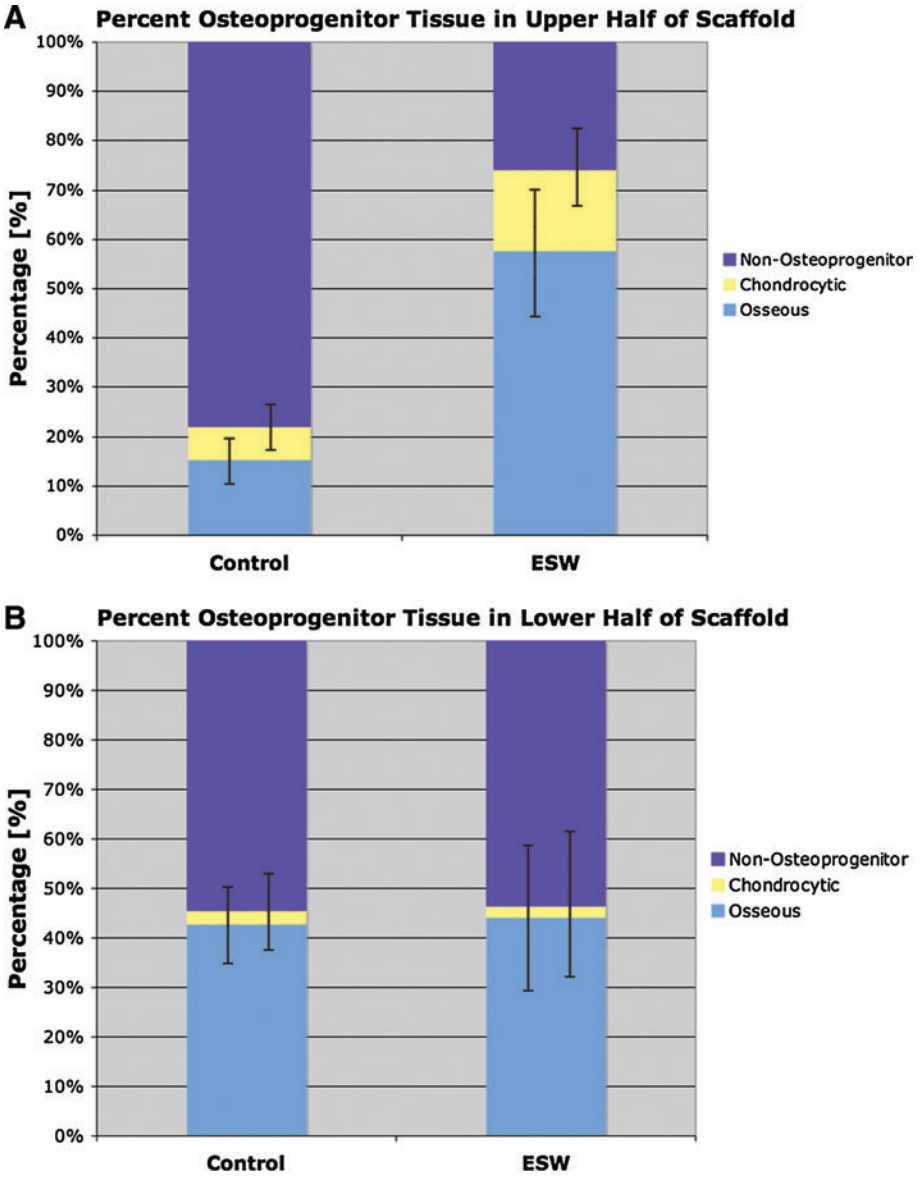

FIG. 4. Graphs of osseous and osteoprogenitor tissue **(A)** within the upper, and **(B)** lower, half of the scaffold for control and ESWSP groups ($n=6$ for controls, 5 for ESWSP; mean ± SEM). Color images available online at www.liebertonline.com/tea

To further examine the ability of ESWSP to generate bone after surgery, the area above the scaffold and the total callus area were recorded. The ESW-treated sample demonstrated a two-fold increase in the callus total area, when compared with controls ($23 \pm 4 mm^2$ vs. $12 \pm 0.3 mm^2$; $p=0.02$). This increase in callus area was a combination of the slightly higher periosteal callus on either side of the implant, as well as the larger amount of periosteal osteoprogenitor tissue above the scaffold. There was a twelve-fold increase in osseous tissue for the total area per unit scaffold length ($0.578 \pm 0.15\, mm^2$/mm scaffold vs. $0.047 \pm 0.04\, mm^2$/mm scaffold; $p=0.005$). With the chondrocytic tissue also considered, the total area of osteoprogenitor tissue was increased by eight-fold for ESW compared with controls ($1.06 \pm 0.35\, mm^2$/mm scaffold vs. $0.13 \pm 0.05\, mm^2$/mm scaffold; $p=0.017$).

Discussion

The primary objective of this study was to demonstrate, using a rabbit model, the effectiveness of a strategy that combines ESW with a bioactive scaffold for orthotopic bone generation. The strategy is based on the ability of ESWs, which are a non-invasive and inexpensive treatment, to rapidly proliferate periosteal cambium layer cells. The ability of ESWs to stimulate periosteal cell proliferation has previously been shown by our group[19] as well as others.[21,22] To our knowledge, to date, however, ESWSP (or ESW-stimulated tissue from any region) has not been combined with scaffolds in a tissue-engineering approach. The advantage of adding a scaffold is three-fold: It contours the new bone, helps maintain bone at the implant site, and creates a space that allows the periosteal cells to further proliferate and fill the scaffold. In this study, ESWSP was overlaid on a porous calcium phosphate scaffold, which had previously been subperiosteally implanted and demonstrated bone formation.[20]

Groups 1 and 2 were used to evaluate and quantify the cambium cell response to ESWs (no scaffold). Animals were sacrificed at the proposed periosteal elevation timepoint (4 days post-ESW); our work, as well as others, shows that at 4

days, the periosteal cells have maximally proliferated but not yet undergone complete osteogenesis.[19,21,22] The ESW treatment site (medial proximal tibia) was chosen, as it is the clinically preferred location of periosteal harvest,[14,23] and we previously demonstrated that tibial periosteal cells are more responsive to ESW stimulation when compared with the femur.[19] There was a significant 2.7-fold increase in the cambium cell number and a significant 4-fold increase in cambium layer thickness; there was also immature bone formation within the proliferated periosteum as previously described.[19,21,22] The advantage of the proliferated cell layer is two-fold. First, it is proposed that the increased progenitor cell number will result in increased callus formation and increased osteogenesis within the scaffold. Second, the thickened layer facilitates harvest. It will be instructive in future studies to evaluate the effects of other values for the energy flux density, number of shocks, and the number and timing of shock sessions on the periosteal cell proliferation. In order to optimize the treatments and the timing of this approach, the detailed temporal response of periosteal cells to ESWs should be examined that would look at cell phenotype, mitosis, and differentiation.

When a calcium phosphate (anorganic bovine bone) scaffold was implanted below the periosteum, there was a 4-fold increase in osseous tissue in the upper half of the scaffold, and a 3.3-fold increase in osteoprogenitor (osseous plus chondrocytic) tissue filling the scaffold upper pores. The increased filling in the scaffold upper pores was attributed to the increased periosteal cell number after ESW stimulation. These cells produced a significant 12-fold increase in the osseous tissue above the scaffold and an 8-fold increase in osteoprogenitor tissue compared with the controls, and the upper pores of the scaffold were filled with 74% osteoprogenitor tissue. For the majority of control samples, there was negligible osteoprogenitor tissue above the scaffold ($0.13 \pm 0.05\,mm^2/mm$ scaffold), which is attributed to the very low periosteal cell number in normal periosteum and the difficulty in their successful harvest. By extension, there was little filling of the upper pores of the scaffold for the CP group ($22\% \pm 5\%$).

After ESW stimulation, the periosteal cells respond by proliferating and undergoing ossification. At the time of a surgery, there is a second stimulus for periosteal proliferation/osteogenesis; previous authors have demonstrated that a normal periosteum responds to surgical elevation by proliferating and undergoing endochondral ossification.[11,17] In this study, both micro-CT and histology show that normal and ESWSP groups undergo callus formation in response to surgical elevation outside the scaffold boundary of both groups (yellow arrows, Fig. 3). In group 4 (ESWSP+ surgery), the cells proliferate more (there is a much thicker layer of subperiosteal tissue in group 4 when compared with group 2 [ESWSP, no surgery]), and they form both bone and cartilage. Our work in rats demonstrated that the cells respond by intramembranous ossification after ESW stimulation[19]; other authors have reported not only primarily intramembranous ossification but also endochondral ossification in rats and rabbits.[21,22] In this study, none of the group 2 ESWSP samples demonstrated endochondral ossification; however, endochondral ossification appeared to be the dominant mechanism of bone formation for group 3, and there was active endochondral ossification in group 4. During surgical manipulation of the periosteum, vessels are damaged, and this causes bleeding. The disruption of the vascular system, coupled with the further proliferation of the cambium cells, likely leads to a hypoxic environment, which is known to favor cartilage formation. That the periosteal cells maintain their chondrogenic potential after ESW stimulation suggests that ESWSP can also be used as a cell source for cartilage repair strategies.

The tissue formed in the lower half of the scaffold is attributed to the periosteal cambium cells that are left on the cortical bone surface after ESW stimulation. This was seen in histological sections (particularly evident in the control samples, which have little tissue in the upper pores from the elevated periosteal cells) as osseous tissue infiltrating the scaffold from below, which was continuous with the cortical bone surface. The lower half of the scaffold was filled equally for both groups (ESW vs. control) with osseous ($\sim$44%) and osteoprogenitor tissue ($\sim$46%). This demonstrates that the periosteal response to the ESW stimulus is a one-time event and that the cells are not permanently altered to a more proliferative state, which is important from a safety viewpoint.

Although ESWs have received a lot of attention and are routinely used in the clinic, the mechanisms underlying the tissue/organ responses to ESWs have not been fully elucidated. It has been reported that ESWs can induce microdamage and initiate a regenerative response, but the molecular and cellular mechanisms of this are still not fully known.[24,25] For the periosteum, some studies have suggested that subperiosteal separation may contribute to periosteal bone apposition,[21,22,26] but another study compared it with surgical periosteal separation alone and found increased osteogenesis in the ESW group.[27] Other mechanisms that have been indentified include increased regional blood flow and/or the release of angiogenic factors[25,27,28]; recruitment and differentiation of MSCs, possibly resulting from marrow hypoxia[25,28,29]; and upregulation of osteogenic factors (e.g., bone morphogenetic proteins, vascular endothelial growth factor).[30–32]

In rat ESW studies, microfractures have not been reported[19,22]; however, here the rabbit model demonstrated cortical microfractures on the side opposite to the application site (postero-lateral corner), which other authors have reported for rabbit bone.[21,26] It is noted that the treatment levels are consistent with current clinical protocols, and it is possible that there is something specific about the bone properties and the biomechanics of shock wave propagation in the rabbit which results in them being more susceptible to ESW-induced microfractures. In horse models, there have been differing reports regarding the induction and exacerbation of microfractures.[27,33] Before the clinical adoption of the technique, these microfractures should be investigated further in large animal models that mimic human anatomy and physiology.

A single timepoint was used to evaluate the rabbit response to bone formation. The 2 week timepoint was chosen based on numerous studies that demonstrated complete osteogenesis at this timepoint after ESW in rabbits,[21,26] and after periosteal elevation in rabbits[11,18] and goats.[17] Further, since our model is at a site that is minimally load bearing, stress-induced remodeling would complicate the observed bone formation if longer timepoints were evaluated. There is

a more pronounced increase in osseous tissue when compared with chondrogenic tissue at the 2 week timepoint post-ESW. A previous work has suggested an angiogenic effect of ESWs and a resulting tendency for intramembranous (not endochondral) bone formation after ESW.[19,22] It is difficult to fully assess this at a single timepoint post-ESW, especially with the complication of surgery. Future works will examine the time course of vessel development and ossification after ESW.

Retraction of the periosteum was observed, although coverage was typically >75%. A model that mimics bone regeneration at a physiologically desired site (e.g., concavity in the bone) would have more periosteum for bone coverage, and, at the same time, allow for evalutation of the remodeling at a load-bearing site. At longer timepoints, the periosteally formed bone is found to undergo maturation[11,18,26]; in our results, the osteoprogenitor tissue was at various phases of endochondral ossification and is expected to undergo complete osteogenesis.

The ESW-stimulated samples outperformed the control group in all key outcome variables (e.g., osteoprogenitor tissue in the upper half of the scaffold, osteoprogenitor tissue above scaffold, callus size). The increased cambium cell number in the ESWSP generated more osteoprogenitor and osseous tissue above the scaffold, and these cells were infiltrating the upper pores of the scaffold and filling them with osteoprogenitor and osseous tissue. This study demonstrates a novel approach for the treatment of bone loss, which has the potential for many clinical situations where bone apposition is required (e.g., vertical ridge augmentation, regrowing bone after tumor resection, and regenerating bone lost at sites of osteolysis). When planning for the implementation of such ESW treatments in human subjects, it will be important to consider species differences in the dose response to ESWs. The doses employed in this and other rabbit studies and in other animal models can serve as guides to the dose (energy flux density, number of shocks, timing of treatment, etc.) to initially be employed for a specific application. Variations among species in the response of a selected tissue site to ESWs can be due to factors including cellularity (number density and types of cells), vascularity, and matrix properties and acoustic impedance mismatches between tissues that would affect shock wave propagation.

Acknowledgments

The research reported here was supported by the U.S. Department of Veterans Affairs, Veterans Health Administration, Rehabilitation Research and Development Service. The authors would like to acknowledge SANUWAVE Health, Inc. (Alpharetta, GA) and Geistlich Pharma (Wolhusen, Switzerland) for providing equipment and materials, respectively, for this project.

Disclosure Statement

There are no conflicts of interest for any of the authors.

References

1. Trueta, J. The role of the vessels in osteogenesis. J Bone Joint Surg Br **45,** 402, 1963.
2. Bruder, S., and Fox, B. Tissue engineering of bone—cell based strategies. Clin Orthop Relat Res **367 Suppl,** S68, 1999.
3. Burg, K.J., Porter, S., and Kellam, J.F. Biomaterial developments for bone tissue engineering. Biomaterials **21,** 2347, 2000.
4. Hutmacher, D. Scaffolds in tissue engineering bone and cartilage. Biomaterials **21,** 2529, 2000.
5. Laurencin, C.T., Ambrosio, A.M., Borden, M.D., and Cooper, J.A. Tissue engineering: orthopedic applications. Annu Rev Biomed Eng **1,** 19, 1999.
6. Muschler, G., Nakamoto, C., and Griffith, L. Engineering principles of clinical cell-based tissue engineering. J Bone Joint Surg **86,** 1541, 2004.
7. Vermeeren, J., Wismeijer, D., and Waas, M. One-step reconstruction of the severely resorbed mandible with onlay bone grafts and endosteal implants: a 5-year follow-up. Int J Oral Maxillofac Surg **25,** 112, 1996.
8. Langer, R., and Vacanti, J. Tissue engineering. Science **260,** 920, 1993.
9. Arnsdorf, E.J., Jones, L.M., Carter, D.R., and Jacobs, C.R. The periosteum as a cellular source for functional tissue engineering. Tissue Eng Part A **15,** 2637, 2009.
10. Choi, Y.-S., Noh, S.-E., Lim, S.-M., Lee, C.-W., Kim, C.-S., Im, M.-W., *et al.* Multipotency and growth characteristic of periosteum-derived progenitor cells for chondrogenic, osteogenic, and adipogenic differentiation. Biotechnol Lett **30,** 593, 2008.
11. Cohen, J., and Lacroix, P. Bone and cartilage formation by periosteum; assay of experimental autogenous grafts. J Bone Joint Surg Am **37,** 717, 1955.
12. Hutmacher, D., and Sittinger, M. Periosteal cells in bone tissue engineering. Tissue Eng **9,** 45, 2003.
13. De Bari, C., Dell'Accio, F., Vanlauwe, J., Eyckmans, J., Khan, I., Archer, C., *et al.* Mesenchymal multipotency of adult human periosteal cells demonstrated by single-cell lineage analysis. Arthritis Rheum **54,** 1209, 2006.
14. O'Driscoll, S. Technical considerations in periosteal grafting for osteochondral injuries. Clin Sport Med **20,** 379, 2001.
15. Mizuno, H., Hata, K., Kojima, K., Bonassar, L., Vacanti, C., and Ueda, M. A novel approach to regenerating periodontal tissue by grafting autologous cultured periosteum. Tissue Eng **12,** 1227, 2006.
16. Reinholz, G.G., Fitzsimmons, J.S., Casper, M.E., Ruesink, T.J., Chung, H.W., Schagemann, J.C., *et al.* Rejuvenation of periosteal chondrogenesis using local growth factor injection. Osteoarthr Cartilage **17,** 723, 2009.
17. Simon, T., Van Sickle, D., Kunishima, D., and Jackson, D. Cambium cell stimulation from surgical release of the periosteum. J Orthop Res **21,** 470, 2003.
18. Stevens, M., Marini, R., Schaefer, D., Aronson, J., Langer, R., and Shastri, V. *In vivo* engineering of organs: the bone bioreactor. Proc Natl Acad Sci U S A **102,** 11450, 2005.
19. Kearney, C.J., Lee, J.Y., Padera, R.F., Hsu, H.-P., and Spector, M. Extracorporeal shock wave-induced proliferation of periosteal cells. J Orthop Res **29,** 1536, 2011.
20. Simion, M., Rocchietta. I., Kim, D., Nevins, M., and Fiorellini, J. Vertical ridge augmentation by means of deproteinized bovine bone block and recombinant human platelet-derived growth factor-BB: a histologic study in a dog model. Int J Periodont Restor Dent **26,** 415, 2006.
21. Tischer, T., Milz, S., Weiler, C., Pautke, C., Hausdorf, J., Schmitz, C., *et al.* Dose-dependent new bone formation by extracorporeal shock wave application on the intact femur of rabbits. Eur Surg Res **41,** 44, 2008.

22. Takahashi, K., Yamazaki, M., Saisu, T., Nakajima, A., Shimizu, S., Mitsuhashi, S., *et al.* Gene expression for extracellular matrix proteins in shockwave-induced osteogenesis in rats. Calcif Tissue Int **74,** 187, 2004.
23. Brittberg, M., Lindahl, A., Nilsson, A., Ohlsson, C., Isaksson, O., and Peterson, L. Treatment of deep cartilage defects in the knee with autologous chondrocyte transplantation. N Engl J Med **331,** 889, 1994.
24. Takayama, K., and Saito, T. Shock wave/geophysical and medical applications. Annu Rev Fluid Mech **36,** 347, 2004.
25. Ogden, J.A., Alvarez, R.G., Levitt, R., and Marlow, M. Shock wave therapy (Orthotripsy) in musculoskeletal disorders. Clin Orthop Relat Res **387,** 22, 2001.
26. Delius, M., Draenert, K., Diek, A.Y., and Draenert, Y. Biological effects of shock waves: *in vivo* effect of high-energy pulses on rabbit bone. Ultrasound Med Biol **21,** 1219, 1995.
27. McClure, S.R., Van Sickle, D., and White, M.R. Effects of extracorporeal shock wave therapy on bone. Vet Surg **33,** 40, 2004.
28. Van Der Jagt, O.P., Van Der Linden, J.C., Schaden, W., Van Schie, H.T., Piscaer, T.M., Verhaar, J., *et al.* Unfocused extracorporeal shock wave therapy as potential treatment for osteoporosis. J Orthop Res **27,** 1528, 2009.
29. Chen, Y., Wang, C., Yang, K., Kuo, Y., Huang, H., Huang, Y., *et al.* Extracorporeal shock waves promote healing of collagenase-induced Achilles tendinitis and increase TGF-beta 1 and 1GF-1 expression. J Orthop Res **22,** 854–861, 2004.
30. Wang, F.S., Yang, K.D., Chen, R.F., Wang, C.J., and Sheen-Chen, S.M. Extracorporeal shock wave promotes growth and differentiation of bone-marrow stromal cells towards osteoprogenitors associated with induction of TGF-beta1. J Bone Joint Surg Br **84,** 457, 2002.
31. Tamma, R., Dell, Endice, S., Notarnicola, A., Moretti, L., Patella, S., Patella, V., *et al.* Extracorporeal shock waves stimulate osteoblast activities. Ultrasound Med Biol **35,** 2093, 2009.
32. Hofmann, A., Ritz, U., Hessmann, M.H., Alini, M., Rommens, P.M., and Rompe, J.-D. Extracorporeal shock wave-mediated changes in proliferation, differentiation, and gene expression of human osteoblasts. J Trauma **65,** 1402, 2008.
33. Da Costa Gómez, T.M., Radtke, C.L., Kalscheur, V.L., Swain, C.A., Scollay, M.C., Edwards, R.B., *et al.* Effect of focused and radial extracorporeal shock wave therapy on equine bone microdamage. Vet Surg **33,** 49, 2004.

Address correspondence to:
Myron Spector, Ph.D.
Department of Tissue Engineering, MS 151
VA Boston Healthcare System
150 S. Huntington Ave.
Boston, MA 02130

E-mail: mspector@rics.bwh.harvard.edu

Received: October 12, 2011
Accepted: March 14, 2012
Online Publication Date: May 22, 2012